The University of Sydney
Department of Civil Engineering
Sydney NSW 2006
AUSTRALIA

http://www.civil.usyd.edu.au

Centre for Geotechnical Research
Research Report No. R807

DEEP PENETRATION OF STRIP AND CIRCULAR FOOTINGS INTO LAYERED CLAYS

By

Changxin Wang, BE, ME
John P. Carter, BE, PhD, FIEAust, MASCE

May 2001

DEEP PENETRATION OF STRIP AND CIRCULAR FOOTINGS INTO LAYERED CLAYS

Research Report No R807

Changxin Wang, BE, ME
John P.Carter, BE, PhD, FIEAust, MASCE

The University of Sydney
Department of Civil Engineering
Centre for Geotechnical Research
http://www.civil.usyd.edu.au

ABSTRACT

The bearing behaviour of footings on layered soils has received significant attention from researchers, but most of the reported studies are limited to footings resting on the surface of the soil and are based on the assumption of small deformations. In this paper, large deformation analyses, simulating the penetration of strip and circular footings into two-layered clays, are described. The upper layer was assumed to be stronger than the lower layer. The importance of large deformation analysis for this problem is illustrated by comparing the small and large deformation predictions. The bearing behaviour is discussed and the undrained bearing capacity factors are given for various cases involving different layer thicknesses and different ratios of the undrained shear strengths of the two clay layers. The development of the plastic zones and the effect of soil self-weight on the bearing capacity are also discussed in the report.

Keywords: large deformation, penetration, strip footing, circular footing, layered clays, bearing capacity

Copyright Notice

Department of Civil Engineering, Research Report R807
Deep penetration of strip and circular footings into layered clays

cxwang@civil.usyd.edu.au
J.Carter@civil.usyd.edu.au

Published by:
Department of Civil Engineering
The University of Sydney
Sydney, NSW, 2006
AUSTRALIA

http://www.civil.usyd.edu.au

1 INTRODUCTION

Natural soils are often formed in discrete layers. For the purpose of analysis it may be convenient and reasonable to assume that the soil within each layer is homogeneous. If a footing is placed on the surface of a layered soil and the thickness of the top layer is large compared with the width of the footing, the bearing capacity of the soil and the displacement behaviour of the footing can be estimated to sufficient accuracy using the properties of the upper layer only. However, if the thickness of the top layer is comparable to the footing width, this approach introduces significant inaccuracies and is no longer appropriate. This is because the zone of influence of the footing, including the potential failure zone, may extend to a significant depth, and thus two or more layers within that depth range will affect the bearing behaviour of the footing. Examples include offshore foundations of large physical dimensions, strip footings or unpaved roads on soft clays.

For strip or circular footings on two-layered clay soils, the bearing capacity usually depends on the ratio of the cohesion (undrained shear strength) of the top layer to that of the lower layer, *i.e.*, c_1/c_2, and the ratio of the thickness of the top layer to the footing width or diameter, *i.e.*, H/B. The literature dealing with bearing capacity of footings is quite extensive. Methods for calculating the bearing capacity of multi-layer soils range from averaging the strength parameters (*e.g.*, Bowles, 1988), using limit equilibrium considerations (Button, 1953; Reddy and Srinivasan, 1967; Meyerhof, 1974), to a more rigorous limit analysis approach (Chen and Davidson, 1973; Florkiewicz, 1989; Michalowski and Shi, 1995). Semi-empirical approaches have also been proposed based on experimental studies (*e.g.*, Brown and Meyerhof, 1969; Meyerhof and Hanna, 1978). The Finite Element Method, which can handle very complex layered patterns, has also been applied to

this problem. (*e.g.*, Griffiths, 1982; Love *et al*., 1987; Burd and Frydman, 1997; Merifield, *et al*., 1999).

However, almost all of these studies are limited to footings resting on the surface of the soil and are based on the assumption that the displacement of the footing prior to attaining the ultimate load is very small. These solutions may be applied to a footing that partially penetrates the soil, by ignoring the strength contribution of the material above the level of the footing base and the change in thickness of the top layer of soil during footing penetration. In some cases, such as those where the underlying soil is very soft, the footings will experience significant settlement, and sometimes even penetrate through the top layer into the deeper layer. In these cases, the small displacement assumption is no longer appropriate, and a large displacement theory should be introduced into the analysis.

If finite deformations are considered in the analysis, a complex interaction of a number of effects occurs. As illustrated in Figure 1, when the footing penetrates into the stronger top layer of a two-layered deposit, the thickness of the upper layer actually decreases as soil is squeezed laterally from under the footing. In addition, footing penetration causes some of the material of the stronger top layer to be trapped beneath the footing so that it is forced into the underlying weaker material. Footing penetration will also cause soil heave close to the footing edges. All these factors will affect the bearing response of the layered soil and in many cases render as inappropriate solutions for the bearing response that are based on small strain theory. On the other hand, large deformation analyses, such as those employing the finite element method, make no *a priori* assumptions about the failure mechanism, and thus they can reflect the natural development of the failure zone and give good predictions of the bearing behaviour.

A large deformation analysis therefore was employed in this paper to predict the behaviour of rigid strip and circular footings penetrating into two-layered clays. In all cases the upper layer is at least as strong or stronger than the lower layer. The bearing behaviour of layered soils at large footing penetrations is specifically investigated.

2 ANALYSIS APPROACH AND FINITE ELEMENT MODELS

For large deformation or large strain analysis, it is well known that the two main approaches are the Eulerian and Lagrangian formulations. Traditionally, large deformation problems in solid mechanics have been solved numerically by the finite element method using a Lagrangian method, as the governing equations in this method are relatively simple and the material properties, boundary conditions, and stress and strain states can be accurately defined. However, in many cases after moderate deformation occurs, the mesh-updating process implicit in most Lagrangian approaches will cause the finite element meshes to become highly distorted or even entangled, and the resulting element shapes may yield negative volumes. This affects the accuracy of the finite element analysis and sometimes makes it impossible to continue.

To circumvent the inaccuracy caused by the excessive mesh distortion in the finite element large deformation analysis, a more flexible approach, called the Arbitrary Lagrangian-Eulerain (ALE) method, has been developed by Ghosh and Kikuchi (1991). Hu and Randolph (1996) also developed a large deformation approach, falling essentially within the ALE category, and their method has been adopted in this paper.

In the method of Hu and Randolph, an infinitesimal strain model is combined with fully automatic mesh generation and plane linear stress interpolation techniques.

Remeshing and interpolation of historical variables are carried out after a specified number of load steps, typically every 10-20 steps. After large deformation occurs and the soil boundary becomes irregular, the re-generated mesh is made to fit the boundary of arbitrary shape very well, and excessive mesh distortion is successfully prevented. Hu and Randolph (1996, 1998) have used this remeshing method to analyse large deformation problems of footings on a single-layered soil as well as the problem of spudcan footing penetration. For the large deformation analyses described in this paper, modification was made to the algorithm developed by Hu and Randolph, to cater for two-layered soils. The modified algorithm was used to generate the finite deformation predictions presented in this paper. Conventional small deformation analyses were also carried out for most of the problems considered here. These were conducted using the AFENA finite element package developed by Carter and Balaam (1995).

In the finite element method, the soil domain is subdivided into a mesh of discrete elements. The meshes used for the present footing problems were designed such that the elements were generally concentrated in the most highly stressed zones. The boundaries of the mesh were sufficiently distant from the footing to ensure that the mesh always contained the entire plastic zone, and this zone did not extend to the mesh boundaries. To ensure that the discretization errors were small in these analyses, several trial calculations were conducted using meshes of different refinement with various load increment sizes. A portion of a typical mesh configuration finally adopted to compute the results presented in this paper is shown in Figure 2. The complete vertical section modelled covers a region that is 20 times the footing width in both breadth and depth.

The loading of a rigid footing was simulated by specifying incremental displacements of the appropriate surface nodes. The displacement increment size was generally taken as 0.02% of the footing width or diameter. The footing base

and sides were assumed to be perfectly smooth. While for the small deformation analysis the mesh configuration always remains the same, in the large deformation analysis the mesh was updated after a specified number of steps of penetration. In the analyses described in this paper, the mesh was updated every 20 steps, and this means that the update interval corresponds to a footing displacement equivalent to 0.4% of the footing width or diameter.

Due to the large number of kinematic constraints imposed on the incremental displacement field as collapse is approached in a constant volume material, the calculation of the bearing capacity becomes very difficult for the displacement finite element method. Reduced or selective integration procedures are often adopted to reduce the detrimental effect of these constraints (Sloan and Randolph, 1982; Burd and Frydman, 1997). Alternatively, higher order elements are employed. In this paper, six-noded triangular elements with a three-point Gauss integration rule were adopted. According to Sloan and Randolph (1982), this linear strain triangular element is suitable for predicting collapse loads accurately for plane strain problems, but for axisymmetric problems they suggested that cubic strain triangles should be used. However, in a recent study of circular foundations (Hu and Randolph, 1998), it was found that good agreement between linear strain and cubic strain triangle solutions could be obtained, if the radius of the circular foundation in the linear strain triangle solution was notionally extended by half an element beyond the 'forced' nodes (the displacement controlled nodes representing the foundation). Thus, following Hu and Randolph, in the present analyses linear strain triangles were used for both strip and circular footings, with the 'effective footing radius' concept adopted in the solution for circular footings, instead of the real radius.

In all cases considered, the soil was assumed to be an elastic-perfectly plastic Tresca material. The rigidity index adopted was $G_1/c_1 = G_2/c_2 = 67$, where G_1, G_2,

c_1 and c_2 are the shear modulus and cohesion of the top and the bottom layers, respectively. Undrained analysis was carried out by adopting a value of Poisson's ratio numerically close to ½, *viz.*, $\nu = 0.49$. The top layer was assumed to be stronger than the bottom layer, and the ratio of the bottom layer strength (c_2) to the top layer strength (c_1) was varied over selected values, *i.e.*, 0.1, 0.2, 1/3, 0.5, 2/3, 0.8 and 1. The ratio of the thickness of the top layer (H) to the footing width or diameter (B) was selected from the values 0.25, 0.5, 1 and 2.

3 BEARING CAPACITY FACTORS PREDICTED BY SMALL DEFORMATION ANALYSIS

3.1 Strip footings

In the absence of a surcharge pressure, the ultimate bearing capacity, q_u, of a strip or circular footing on a two-layered, purely cohesive soil can be expressed as:

$$q_u = c_1 N_c \qquad (1)$$

where N_c is the modified bearing capacity factor that will depend on the strength ratio of the two layers, c_2/c_1, and the relative thickness of the top layer, H/B.

Several researchers have published approximate solutions for the bearing capacity factor N_c for the case of a two-layered soil. For a strip footing, Button (1953) and Reddy and Srinivasan (1967) have suggested very similar values for N_c. These were both upper bound solutions to this problem, and at one extreme they returned a bearing capacity factor for a homogeneous soil (considered as a special case of a two-layered soil) of 5.51, *i.e.*, approximately 7% above Prantl's exact solution of $(2+\pi)$. Brown and Meyerhof (1969) published bearing capacity factors based on experimental studies, and their recommendations are in better agreement with the

value of $(2+\pi)$ for the case of a homogeneous soil. Their factors can be expressed by the following equation:

$$N_c = 1.5\left(\frac{H}{B}\right) + 5.14\left(\frac{c_2}{c_1}\right). \qquad (2)$$

with an upper limit for N_c of 5.14 in this case.

Most recently, Merifield *et al.* (1999) calculated the upper and lower bound bearing capacity factors of layered clays under strip footings by employing the finite element method in conjunction with the limit theorems of classical plasticity. Their results were presented in both graphical and tabular form.

The bearing capacity factors given by the present small deformation analysis were compared with the values predicted by the methods published in these previous works. Cases of H/B = 0.5 and 1 were investigated, and the comparisons are shown in Figure 3. It can be seen that the bearing capacity factors given by the present analysis are less than those given by Button's solution (1953), but larger than the empirical values given by Brown and Meyerhof (1969) and the lower bond solution published by Merifield *et al.* (1999). The best agreement obtained was with the upper bound solution given by Merifield *et al*. (1999). For the special case where $c_2/c_1 = 1$, Button's upper bound solution is 7% higher than the exact value of $(2+\pi)$. If Button's bearing capacity factors for all other cases are reduced by 7%, they agree very well with the upper bounds given by Merifield *et al.* (1999) and the results of the present small strain analyses.

The present finite element predictions for strip footings are about 10-15% larger than the empirical values given by the Brown and Meyerhof (1969) formula, Equation (2). Georgiadis and Michalopoulos (1985) also proposed approximate solutions for the same problem based on a limit equilibrium ("slip surface")

technique. Their predictions were also about 10% higher than the values given by Brown and Meyerhof, but agree well with their own finite element results and independent predictions by Giroud et al. (1973). Although it is difficult to be definitive, it is likely that the bearing capacity factors given by Equation (2) are unduly conservative.

Based on the above comparisons, the finite element mesh and solution algorithm used in the analysis can be regarded as suitable, at least for most practical purposes, for solving this problem of the bearing capacity of a strip footing. In the following large deformation analyses, the mesh used for the small deformation analysis was adopted as the initial mesh, and the meshes re-generated during the loading process had similar mesh densities and element configurations.

3.2 Circular footings

The bearing capacity factor N_c for a circular footing on layered soil is defined in a manner similar to that for a strip footing (Eq. 1). The value of N_c also depends on the strength ratio of the two layers c_2/c_1 and the relative thickness of the top layer H/B (the thickness of the top layer divided by the footing diameter).

The number of published studies of circular footings on layered cohesive soil is significantly less than for plane strain footings on layered soils. For the case of weak over strong cohesive soil, bearing capacity factors were given by Vesic (1970), and these factors were obtained by interpolation between rigorous solutions for related problems. The capacity factors were given in the form of charts in the text entitled “Foundation Engineering Handbook” (Winterkorn and Fang, 1975). For strong over weak soil, Brown and Meyerhof (1969) made a study based on model tests, which were confined to surface loadings, using footings with rough bases. They suggested that the analysis assuming simple shear punching around

the footing perimeter would be appropriate, and in this case the bearing capacity factors were given by the following equation:

$$N_c = 3.0(\frac{H}{2B}) + 6.05(\frac{c_2}{c_1}) \quad (3)$$

with an upper limit for N_c of 6.05 in this case.

In the present study, meshes similar to those used for the strip footing analyses (Fig. 2) were adopted, and the footing base and sides were assumed to be perfectly smooth. Note that in order to calculate the bearing capacity factors, the effective radius was used to compute the total load on the footing instead of the actual radius, as described previously. The effective footing radius for the case where H/B = 1 is 0.52B, and for H/B = 0.5 it is 0.515B.

For a smooth circular footing on homogeneous soil, the bearing capacity factor of 5.69 is about 6% lower than the value of 6.05 that applies to a footing with a rough base (Houlsby and Wroth, 1983). Accordingly, it is reasonable to assume that for layered soils the bearing capacity factors for smooth footings are also lower than those for rough footings of the same proportions. The bearing capacity factors given by Equation (3) for rough footings have been reduced by 6% in order to compare them with the bearing capacity factors predicted by the present small deformation analysis for smooth footings (Fig. 4). It can be seen that the two sets of results agree reasonably well at the limit of a homogeneous soil, but for other cases the results of the present analyses are obviously higher than the predictions of Brown and Meyerhof (1969).

4 LARGE DEFORMATION ANALYSIS OF STRIP FOOTINGS

4.1 The bearing response of weightless soils

The bearing response of strip footings on a strong clay layer overlying a weaker clay layer was examined by comparing the results given by the small and large deformation analyses. Various cases corresponding to H/B = 0.5 and 1, and c_2/c_1 = 0.1, 0.2, 1/3, 0.5, 2/3 and 1 (homogeneous soil) were investigated. Initially, the effect of soil self-weight has been ignored, and normalised load-displacement curves for a weightless soil are shown in Figure 5, for cases where H/B = 1.

Typically, the curve given by the small deformation analysis reaches an ultimate value after a relatively small displacement (footing penetration), and these values of footing load have been used to calculate the bearing capacity factors plotted in the graph in Figure 3(b). Generally, the load-displacement curves given by the large deformation analyses are quite different from those given by the small displacement analysis.

For the homogeneous soil (c_2/c_1 = 1), the load-displacement curve continues to rise until an ultimate value is reached. Figure 5(b) indicates the complete curves for homogeneous soils corresponding to various values of G/c. The ultimate bearing capacity for a deep footing in homogeneous soil was investigated by Meyerhof (1951) and Skempton (1951). Skempton's prediction was based on both theoretical and experimental results and can be simply estimated from the equation:

$$N_c = 5\left(1 + 0.2\left(\frac{s}{B}\right)\right) \qquad (4)$$

whenever $s/B < 2.5$, where s is the settlement or penetration of the footing. For $s/B \geq 2.5$, N_c is constant at a value of 7.5. This is slightly less than the rigorous plasticity solution of $(2+2\pi) \sim 8.28$ (*e.g.*, Meyerhof, 1951) for a smooth strip footing at the bottom of an unsupported slot trench. It can be seen from Figure 5(b) that in contrast to the small deformation prediction, the load-displacement curve given by the large deformation analysis varies significantly with the rigidity index, G/c. When G/c = 200, the results of the large deformation analysis agree reasonably well with Skempton's prediction of the bearing capacity factors for various penetration depths.

For cases where a stronger top layer overlies a much weaker bottom layer (*e.g.*, c_2/c_1 = 0.1, 0.2, and 0.5), the overall response is characterised by some brittleness, even though the behaviour of both component materials is perfectly plastic and thus characterised by an absence of brittleness. For these cases, the load-penetration curves given by the large deformation analysis rise to a peak (see Fig. 5(a)), at which point the average bearing pressure is generally lower than the ultimate bearing capacity predicted by the small deformation analysis. With further penetration of the footing into the clay, it appears that the load-displacement curve approaches an asymptotic value. The peak values of average bearing pressure obtained from these curves are defined as the maximum bearing capacity factors given by the large deformation analysis, and the values reached after large penetration are referred to here as the ultimate bearing capacity factors. It is noted that in the small deformation analysis, the maximum and ultimate values of the bearing capacity factor are identical.

It is reasonable to expect that a footing exhibiting a brittle response should ultimately behave much like a deep strip footing buried in the lower clay layer, so that the ultimate value of the average bearing pressure should then be approximately $(2+2\pi)c_2$, where c_2 is the strength of the lower layer. These

theoretical limits are also indicated on Figure 5(a). It seems clear that curves obtained from the large deformation analysis approach closely these limiting values at deep penetrations.

It is also interesting to note that for this problem geometry, H/B = 1, and for c_2/c_1 = 2/3, the maximum and the ultimate bearing capacity factors are very close to each other, and they are slightly larger than the value given by the small deformation analysis. When c_2/c_1 is greater than 2/3, the large deformation curves appear to rise monotonically to their asymptotic ultimate values. For these cases the ultimate values are reached when the footing has penetrated into the bottom layer and the top layer has separated into two distinct parts. Further discussion of this separation phenomenon is given later in this paper.

Analyses for cases corresponding to H/B = 0.5 were also conducted and these gave load-penetration curves of similar general appearance to those shown in Figure 5. In Figure 6 the values of the bearing capacity factors for cases where H/B = 0.5 and H/B = 1 have been plotted against the strength ratio, c_2/c_1. Also plotted in Figure 6 are the bearing capacity factors predicted by the small deformation analysis.

It can be seen from Figure 6(a) that for the case of H/B = 0.5 and $c_2/c_1 \sim 0.45$ to 0.55, and from Figure 6(b) for H/B = 1 and $c_2/c_1 \sim 1/2$ to 2/3, the maximum bearing capacities given by the large deformation analysis and small deformation analysis are quite close to each other. For cases where the lower layer has a strength weaker than the values defined by these ranges, the large deformation analysis predicts maximum values of N_c that are lower than those given by the small deformation analysis. In cases where the bottom layer has strength greater than about 2/3 of that of the top layer, the large deformation analysis predicts maximum values of N_c that are higher than those given by the small deformation

analysis. The reason for these trends in footing behaviour can be explained in terms of the overall deformation mechanism, as follows.

When a rigid footing penetrates a finite distance into a two-layered soil system, the mobilised bearing resistance is derived from at least two significant sources. One is the shear strength of the soil beneath the footing, and the other is the strength and self-weight (if significant) of the soil that is pushed above the level of the footing base. If a small deformation analysis is carried out, only the first component is considered, as it is assumed that the geometry of the problem remains unchanged during the analysis, so that the tendency for soil to heave beside the footing is ignored. For the large deformation analysis, the geometry of the problem is updated regularly and thus the relative contributions to the bearing resistance from the two sources vary continuously during the penetration.

During the early stages of penetration, almost all the soil lies beneath the footing base, and thus the load-displacement curves are almost identical to those given by the small deformation analysis. As the footing penetrates into the soil and plastic yielding increases, the soil of the top layer flows plastically from beneath the footing leading to a thinner top layer of soil immediately beneath the footing. Consequently, the relative contribution to the overall bearing resistance of the stronger top layer reduces as the layer thickness reduces. However, as this thinning occurs more soil is pushed above the level of the footing base. The geometry of the problem changes, and in particular the nature and shape of the zone of material that has reached plastic failure will change. Generally, as the footing penetrates further below the original surface level, more of the soil will be required to yield plastically to accommodate the penetration, and this contributes to an increase in the bearing resistance. In addition, if heave occurs in a gravitational field, greater work will need to be done by the footing to cause a material with self-weight to heave above footing level. The finite penetration of the footing therefore

gives rise to two competing influences on the mobilised bearing resistance. Whether the bearing resistance predicted by the large deformation analysis is higher or lower than that given by the small deformation analysis depends on how these two factors interact.

From these results it is clear that a characteristic value of the strength ratio c_2/c_1 can be identified, at least approximately. For example, when $c_2/c_1 < 0.45$ to 0.55 for the case of H/B = 0.5 and G/c = 200, and when $c_2/c_1 < 0.5$ to 2/3 for the case of H/B = 1 and G/c = 200, the reduction in bearing resistance caused by the plastic flow of the stronger top layer from beneath the footing is always greater than the gain in resistance associated with footing burial and the heave of soil above the level of the footing base. Thus in these cases both the maximum and ultimate bearing capacity factors are lower than those given by the small deformation analysis. Furthermore, in such cases the overall behaviour is characterised by a brittle response. The smaller the value of c_2/c_1, the lower is the predicted bearing resistance at any given value of footing displacement.

In cases where the strength ratio is greater than the characteristic value, the increase in resistance due to burial is always greater than the reduction due to thinning of the top layer, and this leads to a load-displacement curve that continues to rise monotonically. Thus for these cases the maximum bearing capacity factors are approximately the same as the ultimate bearing capacity factors and are always greater than those given by the small deformation analysis, at least for the range of footing penetrations investigated here.

4.2 Large deformation process and development of plastic zones

A graphical representation of the penetration of a strip footing into a two-layered soil is shown in Figures 7(a)-(f), for the case of H/B = 0.5 and $c_2/c_1 = 0.5$. As the

footing penetrates from the surface, the top clay layer is seen to flow gradually out from under the footing, so that the layer becomes thinner locally beneath the footing base, especially under the edge. However, not all of the top layer soil will flow out from under the footing base; some soil will remain trapped under the footing. Thus the top layer of soil tends to break into two parts. One part remains under the footing during further settlement, the other flows to the side of the footing. Numerically, in the remeshing algorithm used for the analysis of layered soil, if the thickness of the top layer of soil at the side of the footing became less than 3% of the footing width, it was arbitrarily assumed that the layer had effectively separated into two parts (*e.g.*, see Figure 7(e) and 7(f), where the enlarged image shows the gap clearly). The footing and the trapped soil subsequently settle together into the bottom layer of soil. From this stage onwards, the value of the mobilised bearing resistance usually does not change much with further penetration. This is because the contribution to the bearing capacity from the two sources identified previously varies very little after this stage, so that a relatively stable value for the ultimate bearing resistance is obtained.

As footing penetration occurs, a zone of plastic failure develops within the soil. In Figures 8(a) and 8(b), well-developed plastic zones are illustrated for the cases where H/B = 1 and $c_2/c_1 = 0.5$ and $c_2/c_1 = 0.1$. With further penetration, the plastic zone develops very slowly and the failure zones shown in Figure 8 change only slightly. It can be seen that when $c_2/c_1 = 0.5$, the plastic zone is restricted to a relatively small area. However, for a very weak lower layer, *e.g.*, $c_2/c_1 = 0.1$, the plastic zone is much more extensive.

Plastic yielding first occurred in the top layer for the case of $c_2/c_1 = 0.5$. Subsequently, the bottom layer began to fail plastically, with yield commencing just beneath the material interface. The failure zone then extended into both layers, but with faster growth with increasing penetration occurring in the bottom layer.

For the case where the bottom layer was very weak, *e.g.*, $c_2/c_1 = 0.1$, failure commenced first in the bottom layer, and only after it developed over a relatively large area within the bottom layer, did failure commence in the top layer. During subsequent footing penetration the plastic zone developed very quickly in the bottom layer. The weaker the bottom layer compared to the top, the more extensive is the plastic zone developed in the bottom layer, as might be expected.

4.3 The effect of H/B

In the above analyses, a range of values of c_2/c_1 has been considered, and their effects on the load-displacement behaviour have been discussed. Two values of H/B, *i.e.*, H/B = 0.5 and 1, have been adopted in these analyses, and it was discovered that their difference did not have a significant effect on the load-displacement behaviour. However, when a wider range of H/B is included in the study, the effect of H/B is more marked.

Figure 9 shows the load-displacement curves for strip footings penetrating into layered soil with $c_2/c_1 = 0.5$, and the value of H/B varied from 0 (homogeneous case with soil cohesion of c_2), 0.25, 0.5, 1, 2, and ∞ (homogeneous case with soil cohesion of c_1). As the footing penetrates into the layered clays with H/B ≤ 1, it is obvious that the load-displacement curves approach the bearing capacity for a deeply buried footing in a clay of strength c_2, *i.e.*, $P/Bc_1 = 0.5(2+2\pi)$. As indicated previously, when H/B = ∞, the load-displacement curve approaches the value of $P/Bc_1 = 2+2\pi$. When $1 < H/B < \infty$, the maximum value of the average bearing pressure of the footing reaches a value between $0.5(2+2\pi)c_1$ and $(2+2\pi)c_1$. However, as the penetration continues, the load-displacement curves are expected to decline, and should eventually approach a bearing capacity factor of $0.5(2+2\pi)c_1$.

Among the curves given in Figure 9, brittle behaviour is shown for the cases where H/B = 0.5, 1 and 2 as the footing penetrates into the bottom layer. For cases where H/B > 2, this brittle behaviour is also expected, although it is not demonstrated in Figure 9. However, for the cases where H/B < 0.5, there is no brittle behaviour shown in the load-displacement curves. For these cases, the top layer is very thin and thus the effect of its higher strength is not sufficient to generate a peak in the load-displacement curves.

4.4 The effect of soil weight

It is well known that for a surface footing on a purely cohesive soil, the ultimate bearing capacity given by the undrained analysis is independent of the soil density. Thus the results given by the small deformation analysis are identical for weightless soils and for soils of the same strength but with self-weight. However, in large deformation analysis, the footing can no longer be regarded as a surface footing once it begins to penetrate into the underlying material, and in this case the self-weight of the soil will also affect the penetration resistance.

The results of all footing analyses presented thus far were obtained without considering the effects of soil self-weight. This was done deliberately in order to investigate the effects of the large deformation analysis exclusively on the bearing capacity factor N_c. However, if soil self-weight is included, the effect of surcharge pressure on the load-displacement behaviour is significant. Figure 10 shows the load-displacement curves for the case where H/B = 1 and c_2/c_1 = 0.2 and 0.5. For these cases, an identical soil unit weight was assumed for both layers ($\gamma_1 = \gamma_2 = \gamma$). These curves show clearly that the soil self-weight tends to suppress the tendency for a brittle system response.

Figure 11 shows the soil surface profiles for a one-metre wide footing with H/B = 1 and $c_2/c_1 = 0.5$ that has penetrated into a two-layered soil to 2.5 metres (The length scales displayed in Fig. 11 have units of cm). Greater surface heave is observed for the case of a weightless soil. In all cases the soil was constrained not to flow over the top surface of the footing.

To investigate the effect of soil self-weight quantitatively, it would seem reasonable to approximate the mobilised bearing resistance, q_m, using the following equations:

$$q_m = c_1 N_{ms} + \gamma_1 s \tag{5}$$

whenever $s \le H$, and

$$q_m = c_1 N_{ms} + \gamma_1 H + \gamma_2 (s - H) \tag{6}$$

whenever $s \ge H$. γ_1 and γ_2 are the unit weights of the upper and lower soil layers, respectively, and s is the settlement (or penetration) of the footing into the underlying soil. The bearing capacity factor N_{ms} is defined as:

$$N_{ms} = \frac{q_{ms}}{c_1} \tag{7}$$

where q_{ms} is the average mobilsed pressure on the footing when the footing penetrates into a weightless soil to a depth s. When $\gamma_1 = \gamma_2$, Equation (6) reduces to Equation (5) for any penetration.

In Figure 12(a), the load-displacement curves shown in Figure 10(a) are compared with the predictions given by Equation (5), and it can be seen that good agreement is achieved for all cases. To investigate further the accuracy of Equations (5) and (6), a layered soil with different densities for the top and bottom layers was also investigated.

In Figure 12(b), load-displacement curves predicted by Equations (5) and (6) are given for the following cases for which H/B = 1 and $c_2/c_1 = 0.5$. Details of the curves indicated on this figure are as follows:

(a) Small deformation analysis for a surface footing,

(b) Large deformation analysis for a footing on a weightless soil,

(c) Large deformation analysis for a footing on a soil with a unit weight of $20kN/m^3$ in both layers,

(d) Large deformation analysis for a footing on a layered soil, where the top layer has a unit weight of $20kN/m^3$ and the bottom layer $15kN/m^3$,

(e) The curve corresponding to case (b) with the ordinate values augmented by $\gamma s/c_1$ where $\gamma = 20kN/m^3$, and

(f) The curve corresponding to case (b) with the ordinate values augmented by $\gamma s/c_1$ when $s \leq H$, or by $\gamma_1 s/c_1+\gamma_2(s-H)/c_1$ when $s > H$, where $\gamma_1 = 20kN/m^3$ and $\gamma_2 = 15kN/m^3$.

It can be seen from Figure 12(b) that for the weightless soil, curve (b) declines after a peak occurs, but in contrast curves (c) and (d) continue to rise, presumably because the effects of the term $\gamma_1 s$ or $\gamma_1 s/c_1+\gamma_2(s-H)/c_1$ are dominant (see Equations 5 and 6).

Curves (c) and (e), and (d) and (f) are compared in Figure 12 to assess whether the relations expressed in Equations (5) and (6) give an adequate estimate of the effects of self-weight on the mobilised bearing resistance. At the early stages of

footing penetration, curves (c) and (d) predict significantly lower bearing resistance than curves (e) and (f). However, curves (c) and (d) predict higher bearing resistance as the penetration continues, but the differences are small. Thus it can be concluded that Equations (5) and (6) may be used to estimate for most practical purposes the influence of soil self-weight on the bearing response in the large deformation range.

5 LARGE DEFORMATION ANALYSIS OF CIRCULAR FOOTINGS

5.1 The bearing response

In this section, the bearing response of circular footings penetrating two-layered soils is examined. As before, it is generally assumed that the overlying layer is stronger than the underlying soil and that each clay layer behaves in an undrained manner, so that it can be modelled as a purely cohesive material. Predictions given by both the small and large deformation analyses are presented. Various cases corresponding to H/B = 0.5 and 1, and c_2/c_1 = 0.1, 0.2, 1/3, 0.5, 2/3 and 1 have been investigated, and typical normalised load-displacement curves are shown in Figure 13.

Comparing the load-displacement responses of strip and circular footings on the same layered soils, overall the large deformation effects generally appear to be more significant for the case of a circular footing (*c.f.*, Figs 5(a) and 13), as the differences between the small and large deformation analyses are generally greater for a circular footing than for the corresponding strip. In Figure 13 it may be observed that the small deformation analysis predicts almost identical bearing responses for layered soils characterised by c_2/c_1 = 0.5 to 1, but the large deformation analysis predicts significantly different behaviour for these cases.

In all cases examined, the maximum bearing capacity factors obtained from the large deformation analysis were greater than those obtained from the small deformation analysis. Both sets of values are plotted in Figure 14. This means that for the problems investigated, and before the maximum bearing capacity is reached in each case, the effect of the increased bearing resistance from the soil above the footing base always has greater significance than the thinning of the stronger top layer immediately beneath the footing. For the large deformation analyses, no obvious ultimate bearing resistance was reached within the range of footing penetration investigated, *i.e.*, up to 5B. In cases where the lower layer is very weak, *i.e.*, $c_2/c_1 = 0.1$ to 0.5, it can be seen in Figure 13 that the predicted bearing behaviour of the footing is much more brittle than that of a strip footing on the same soil. Also indicated on Figure 13 are the ultimate bearing capacities of circular footings embedded deeply in a material with the same strength as the lower clay layer. These values are given by the approximate expression for the ultimate capacity of a cylindrical shaft foundation with perfectly smooth sides (Meyerhof, 1951), *i.e.*, $9.34c_2$. Although most of the finite deformation analyses have not been taken to sufficiently large penetrations to mobilise the ultimate resistance, there is an indication that after the peak in the brittle response some of the curves (*i.e.*, for cases where $c_2/c_1 \leq 2/3$) are tending to approach these respective ultimate limits. However, the present large deformation analysis predicted significantly higher bearing ultimate bearing pressures for cases where $c_2/c_1 = 0.8$ and 1. This inconsistency is possibly caused by using the "effective radius" in calculating the average pressure on the footing. More accurate predictions might be obtained by adopting cubic strain triangle elements instead of the linear strain six-noded triangles used in this study.

5.2 The development of a plastic zone

Figures 15a-c show well-developed plastic zones under the circular footing for cases where H/B = 1 and c_2/c_1 = 0.1, 0.5 and 0.8. It can be seen that the weaker the lower layer relative to the top layer, the more the failure is confined to the lower layer, as might be expected. However, the depth of the plastic zone under a circular footing varies only very slightly with the value of c_2/c_1. Compared to strip footings, the zone of plastic failure is much less extensive for circular footings.

5.3 The effect of H/B and soil weight

The effects of H/B and soil weight on the bearing resistance of circular footings were found to be similar in nature to those predicted for strip footings. The brittle behaviour is not shown for the cases of very small value of H/B, in which the behaviour of a 'quasi-homogeneous' soil with the strength of the bottom layer is dominant. For the cases of very large value of H/B, the brittle behaviour does not occur before a significant penetration happens, *i.e.*, the footing is close to penetrating through the top layer.

When soil density is considered, the bearing capacity is given to sufficient accuracy by Equations (5) or (6), depending on whether or not both layers have the same density. However, in these equations the values of N_{ms} must be replaced by the bearing capacity factors corresponding to the large deformation response of circular footings on weightless soil.

6 CONCLUSIONS

Large deformation analyses were carried out to investigate the bearing response and failure mechanism of a horizontally layered cohesive soil under the action of

vertically loaded rigid strip or circular footings. Cases involving only two different undrained clay layers were considered, and the upper layer was always stronger than the lower layer. Generally, the load-displacement curves predicted by the large deformation analyses were significantly different from the ones given by the small deformation analysis. During footing penetration, at least two major factors affect the bearing response; one is the movement of soil from beneath the footing to a region above the level of the footing base and the other is the influence of the weaker lower layer. Both effects increase with penetration because more soil moves above the footing level and the upper layer is made thinner as it is squeezed from under the footing. Of course these two factors are just different aspects of the same deformation mechanism. The former tends to increase the bearing resistance, while the latter tends to reduce it.

For a strip footing on a two-layered soil with a specified value of H/B, a characteristic value of c_2/c_1 was observed where the two effects can be roughly offset, and the load-displacement curve is almost the same as the one given by the small deformation analysis. For values of c_2/c_1 greater than this characteristic value, the load-displacement curve rises continuously until the footing penetrates into the bottom layer and a stable ultimate bearing capacity is achieved, which is also the maximum bearing capacity. For values of c_2/c_1 smaller than the characteristic value, the curve rises to a maximum bearing capacity, then declines to the ultimate bearing capacity. In most cases the ultimate capacities are very close to the analytical values predicted for a footing deeply buried in the weaker underlying clay layer.

For a strip footing on a two-layered soil with various value of H/B, all the load-displacement curves are expected to approach the bearing resistance of a deeply buried footing in a soil with the strength of the bottom layer. However, for layered soils with large values of H/B, this will happen only when the top layer is close to

being fully penetrated. For layered soils with very small values of H/B, a brittle behaviour does not occur.

For a circular footing on a two-layered soil, the large deformation effects appear to be more significant than for strips. There appears to be no obvious characteristic value of c_2/c_1 obtained where the load-displacement curves given by the small and large deformation analysis are coincident or almost coincident with each other. For cases of c_2/c_1 = 0.1 to 2/3, the load-displacement curves indicate a trend of approaching the ultimate capacity of a footing deeply buried in the lower clay layer. However, for cases of c_2/c_1 = 0.8 to 1, the ultimate bearing capacity given by the present large deformation analyses is higher than the analytical value for a footing buried in the weaker lower layer. It is possible that this inconsistency is caused by using the "effective radius" in calculating the average pressure on the footing. More accurate predictions might be obtained by adopting cubic strain triangle elements instead of the linear strain six-noded triangles. However, these additional calculations are beyond the scope of the work described in this paper. It is noted that the effect of H/B on the behaviour of circular footings is similar in nature to the effect it has for strip footings.

During the strip footing penetration, the failure zone may either develop first in the upper layer (for a relatively large c_2/c_1) or the lower layer (for a relatively small c_2/c_1), but it develops much faster and more extensively in the lower layer. The smaller the value of c_2/c_1, the more extensively the plastic zone developed in the weaker underlying layer. The failure zone under a circular footing is much more restricted than that under a strip footing, and the variation in size of the plastic zone for different values of c_2/c_1 is not very significant.

Although soil self-weight does not affect the predicted bearing response of cohesive soil in a small deformation analysis, it can have a significant influence in

a large deformation analysis. For a two-layered soil of uniform density, the bearing resistance of a strip or circular footing can be roughly predicted by adding an appropriate surcharge value (γs) to the bearing resistance predicted by the analysis that ignores soil self-weight. This prediction usually produces a slight under-estimate of the mobilised resistance for footings at large penetrations.

7 ACKNOWLEDGEMENTS

Support for the research described in this paper was provided by grants from the Australian Research Council, including funding through the Special Research Centre for Offshore Foundation Systems.

8 REFERENCES

Bowles, J.E., (1988), Foundation Analysis and Design, Mcgraw-Hill, New York.

Brown, J. D. and Meyerhof, G. G. (1969), 'Experimental study of bearing capacity in layered clays', Proc., 7th Int. Conf. on soil Mechanics and foundation engineering, Mexico, Vol. 2, pp. 45-51.

Burd, H. J. and Frydman, S. (1997), 'Bearing capacity of plane-strain footings on layered soils, Can. Geotech. J. Vol. 34, pp.241-253.

Button, S. J. (1953), 'The bearing capacity of footings on a two-layer cohesive subsoil', Proc., 3rd Int. Conf. on soil mechanics and foundation engineering, Zurich, Vol.1, pp.332-335.

Carter, J. P. and Balaam, N. (1995), AFENA Users Manual, Geotechnical Research Center, The University of Sydney.

Chen, W.F., and Davidson, H.L. (1973), 'Bearing capacity determination by limit analysis', J. Soil Mech. Found. Div., Vol. 99, No.6, pp.433-449.

Florkiewicz, A. (1989), 'Upper bound to bearing capacity of layered soils', Can. Geotech. J. Vol. 26, pp. 730-736.

Georgiadis, M. and Michalopoulos, A. P. (1985), 'Bearing capacity of gravity bases on layered soil', J. of Geotechnical Eng. Vol. 111. No. 6, pp. 712-727.

Ghosh, S. and Kikuchi, N., (1991), 'An arbitrary Lagrangian-Eulerian finite element method for large deformation analysis of elastic-viscoplastic solid', Comp. Methods Appl. Mech. Eng., Vol. 86, pp.127-188.

Giroud, J. P., Tran-Vo-Nhiem and Obin, J. P. (1973), 'Table pour le calcul des foundations', Tome 3, Force Portante, Dunod, Paris, France.

Griffiths, D.V. (1982), 'Computation of bearing capacity on layered soils', Proc., 4th Int. Conf. on Num Meth. In Geomechanics, Vol. 1, pp.163-170.

Hu, Y. and Randolph, M. F. (1996), 'A practical numerical approach for large deformation problems in soil', Research Report G1226, Dept. of Civil Eng., The Univ. of Western Australia (also available: Int. J. Num. Analy. Meth. Geomechanics., 1998, Vol. 22, pp.327-350).

Hu, Y. and Randolph, M. F. (1998), 'Deep penetration of shallow foundations on non-homogeneous soil', Soils and Foundations, Vol. 38, No. 1, pp.241-246.

Love, J.P., Burd, H.J., Milligan, G.W.E., and Houlsby, G. T. (1987), 'Analytical and model studies of reinforcement of a layer of granular fill on a soft clay subgrade', Can. Geotech. J., Vol. 24, pp.611-622.

Merifield, R. S., Sloan, S. W., and Yu, H.S. (1999), 'Rigorous plasticity solutions for the bearing capacity of two-layered clays', Geotechnique, Vol. 49, No.4, pp.471-490.

Meyerhof, G. G. (1951), 'The ultimate bearing capacity of foundations', Geotechnique, Vol. 2, No.4, pp.301-332.

Meyerhof, G. G. (1974), 'Ultimate bearing capacity of footings on sand layer overlaying clay', Can. Geotech. J., Vol. 11, No. 2, pp. 223-229.

Meyerhof, G.G. and Hanna, A. M. (1978), 'Ultimate bearing capacity of foundations on layered soils under inclined load', Can. Geotech. J., Vol. 15, pp.565-572.

Michalowski, R. L. and Lei Shi (1995), 'Bearing capacity of footings over two-layer foundation soils', ASCE, J. of Geotechnical Engrg. Div., Vol. 121, No. 5, pp. 421-427.

Reddy, A. S., and Srinivasan, R. J. (1967), 'Bearing capacity of footings on layered clays', J. Soil Mech. Found. Div., ASCE, Vol. 93, No. 2, pp. 83-99.

Skempton, A. W. (1951), 'The bearing capacity of clays', Build. Res. Cong., Division 1, Part 3, pp. 180-189, London.

Sloan, S. W. and Randolph, M. F. (1982), 'Numerical prediction of collapse loads using finite element methods', Int. J. Num. Analy. Meth. Geomech. Vol. 6, pp.47-76.

Vesic, A. S. (1970), 'Research on bearing capacity of soils', unpublished reference in 'Bearing capacity of shallow foundations', Foundation Engineering Handbook, 1st edn., H. F. Winterkorn and H. Y. Fang (eds), Chapter 3, Van Nostrand Reinhold, New York.

Winterkorn, H. F. and Fang, H. Y. (eds) (1975), Foundation Engineering Handbook, 1st edn., Van Nostrand Reinhold, New York.

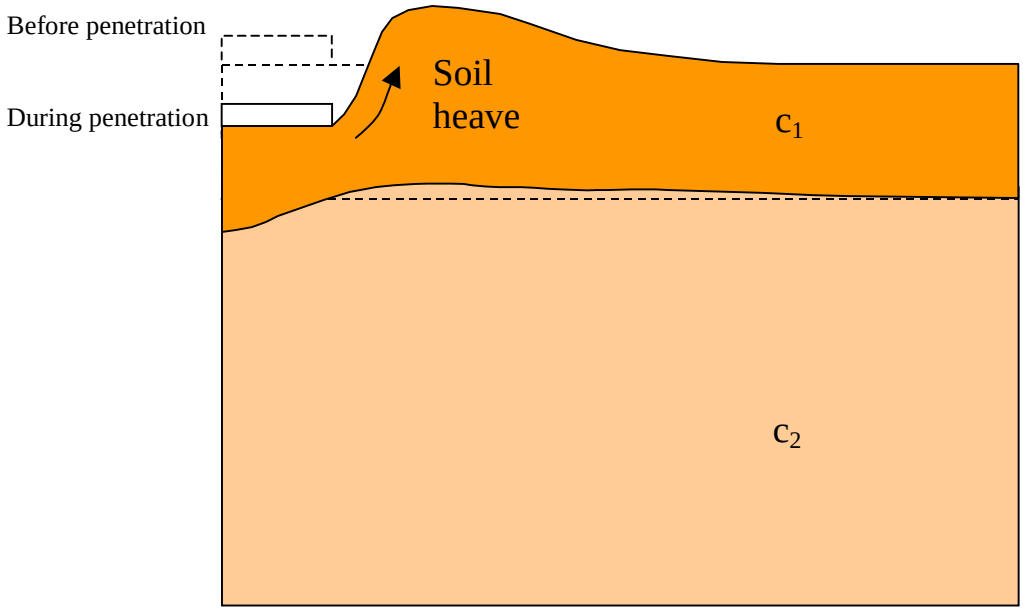

Figure 1 Soil deformation profile as a footing penetrating into two-layered soils

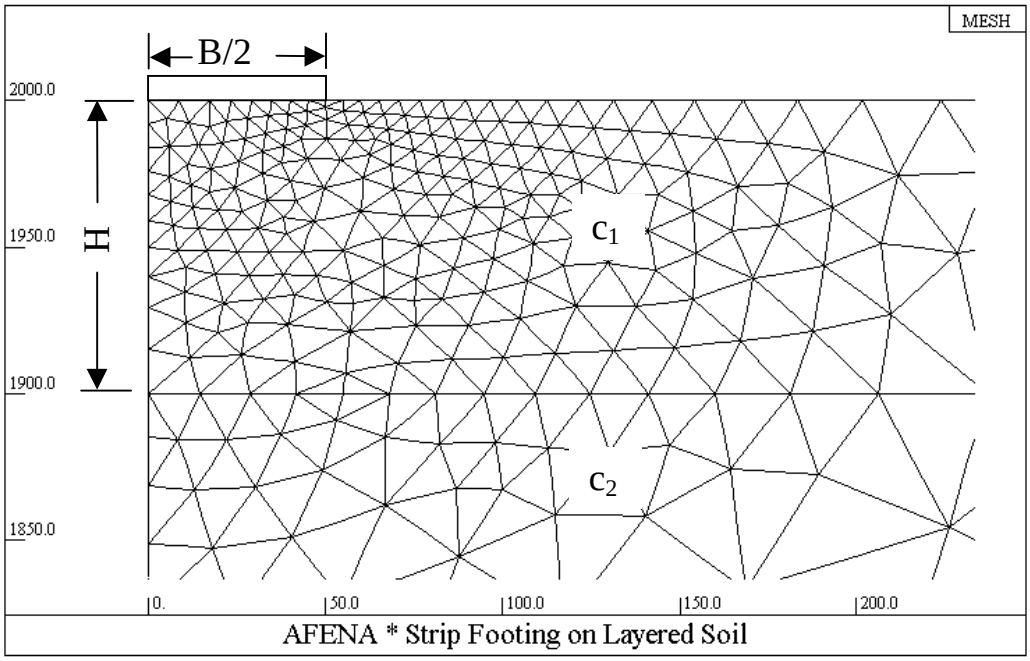

Figure 2 Typical finite element mesh configuration

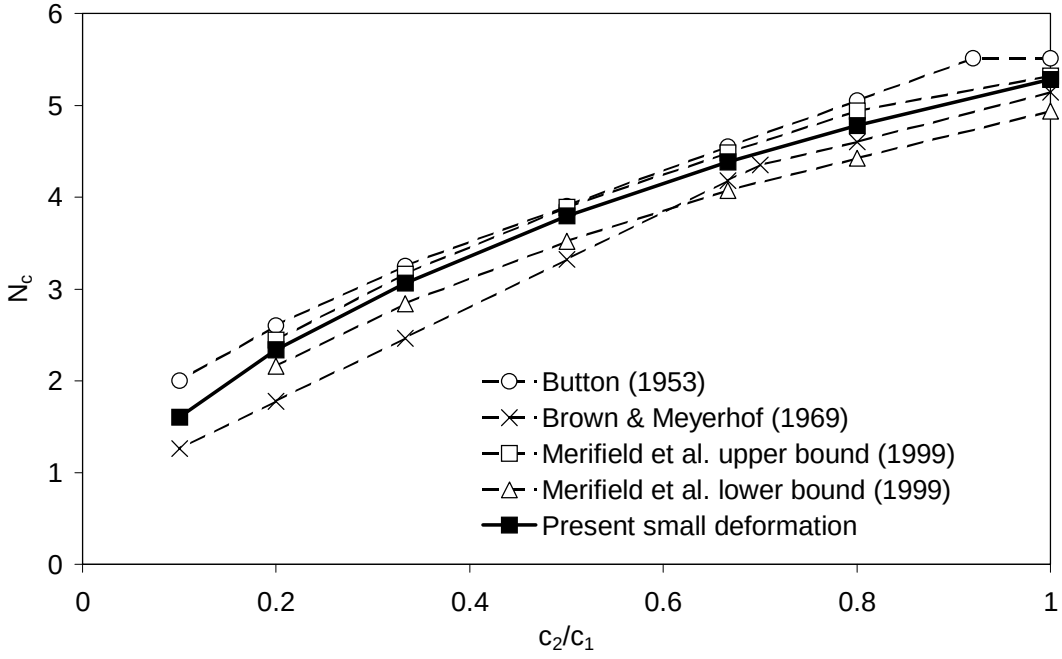

(a) H/B = 0.5

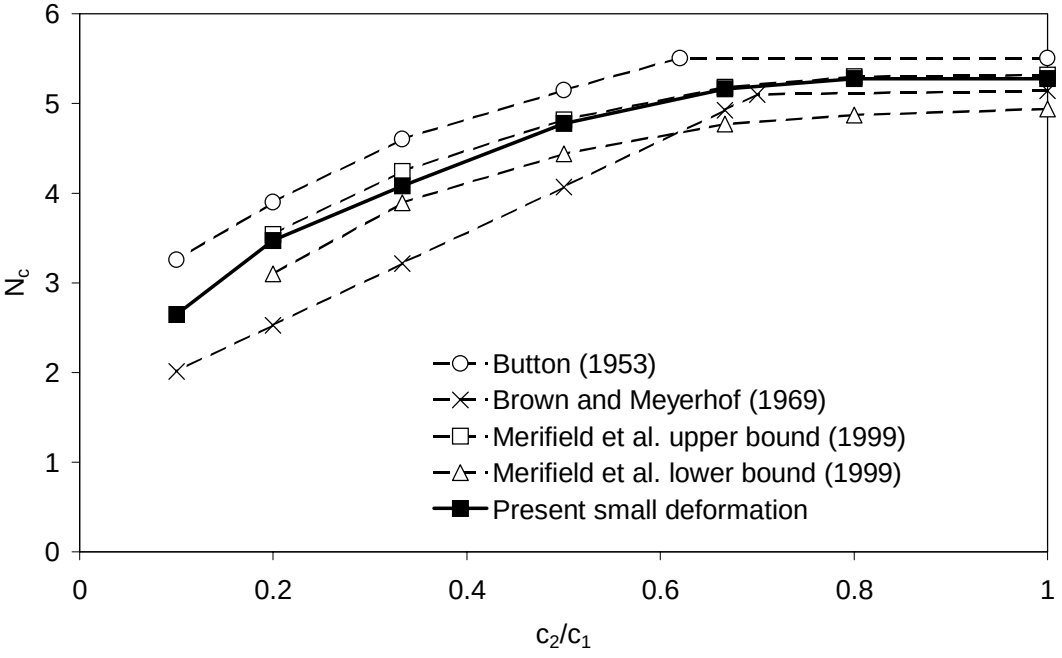

(b) H/B = 1

Figure 3 Bearing capacity factors for a strip footing

(small deformation analysis)

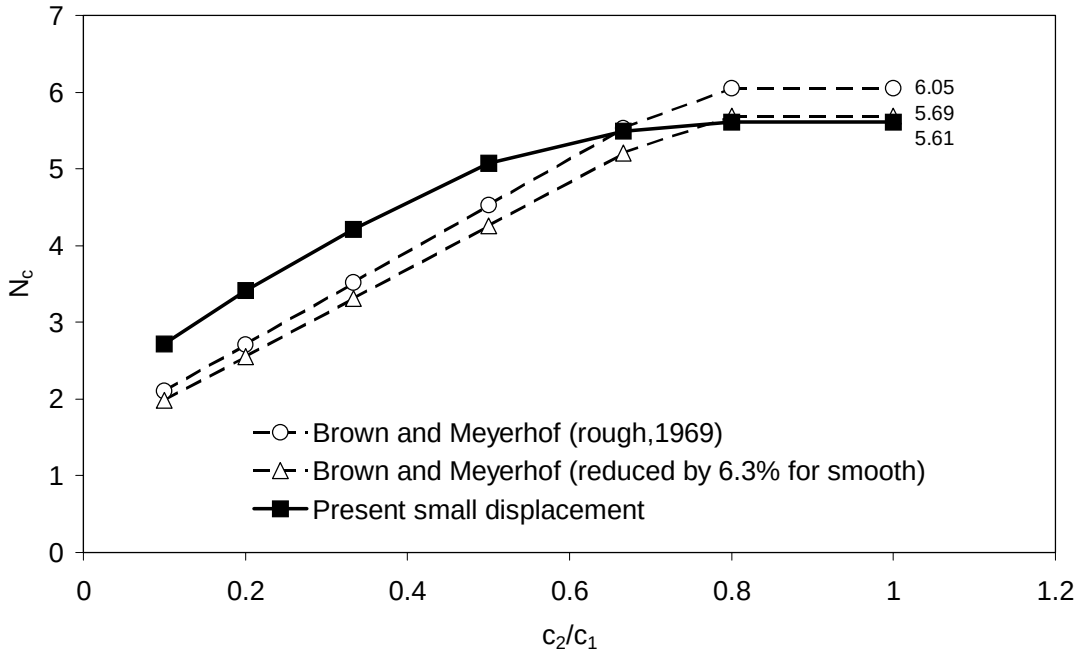

(a) H/B = 0.5

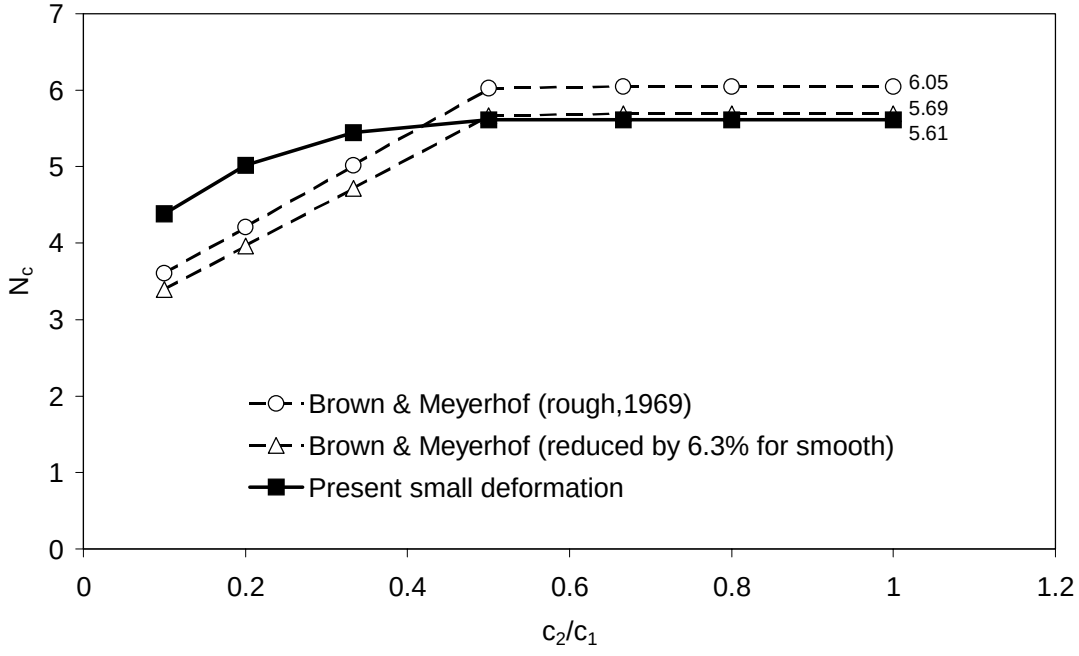

(b) H/B = 1

Figure 4 Bearing capacity factors for a circular footing

(small deformation analysis)

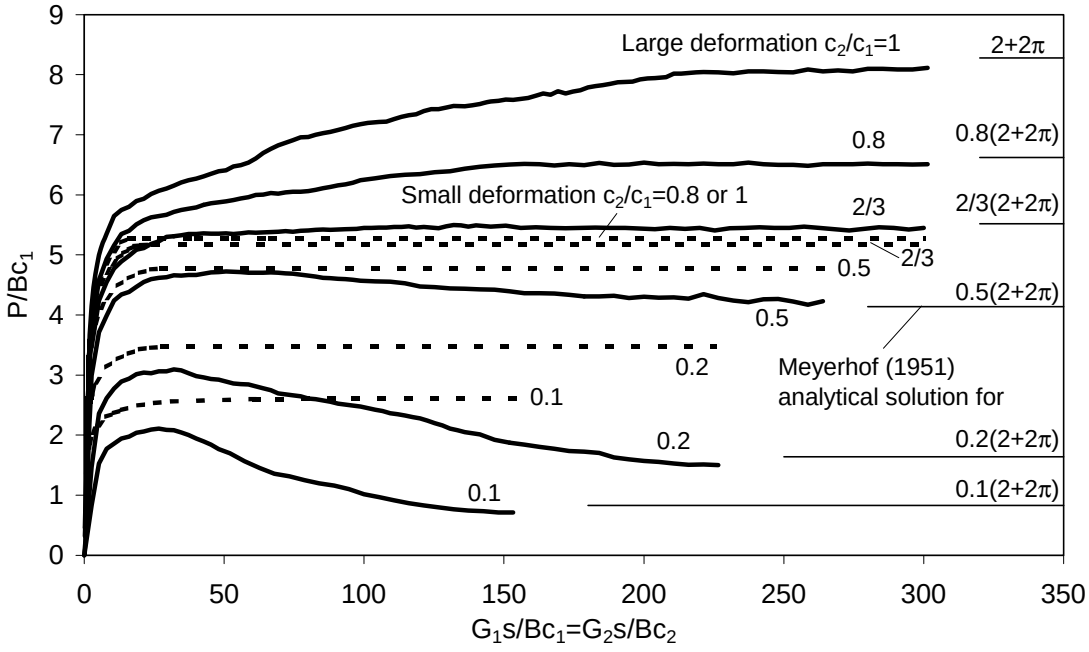

(a) Load-settlement curves for layered clay ($G_1/c_1 = G_2/c_2 = 67$)

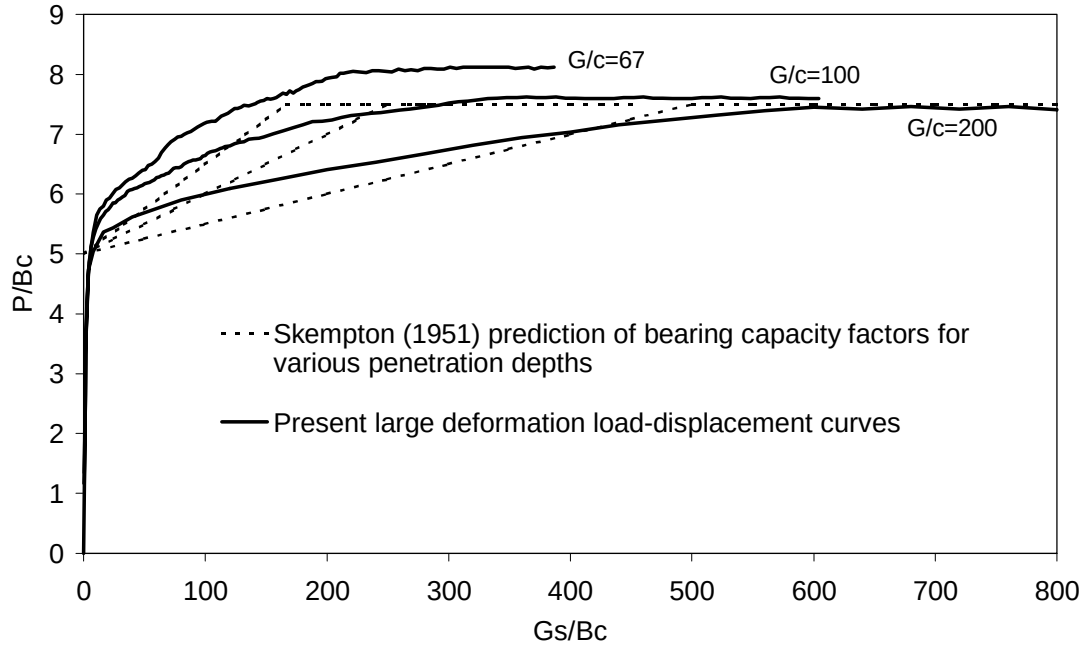

(b) Load-settlement curves for a homogeneous clay

Figure 5 Typical normalized load-settlement curves for a strip footing on homogeneous or layered clay (H/B = 1)

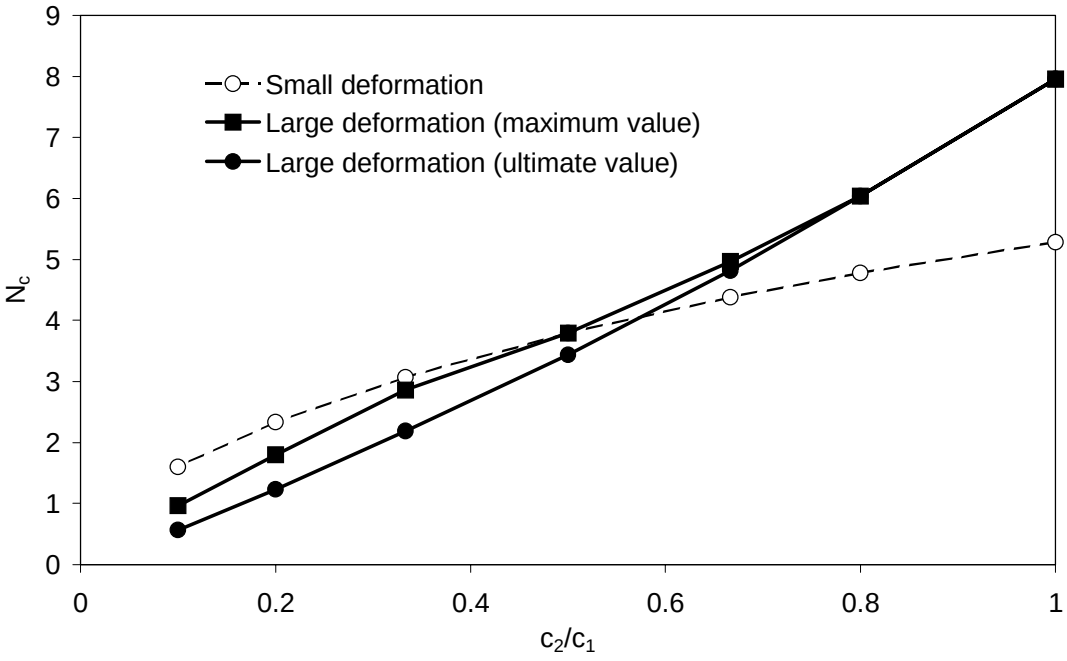

(a) H/B = 0.5

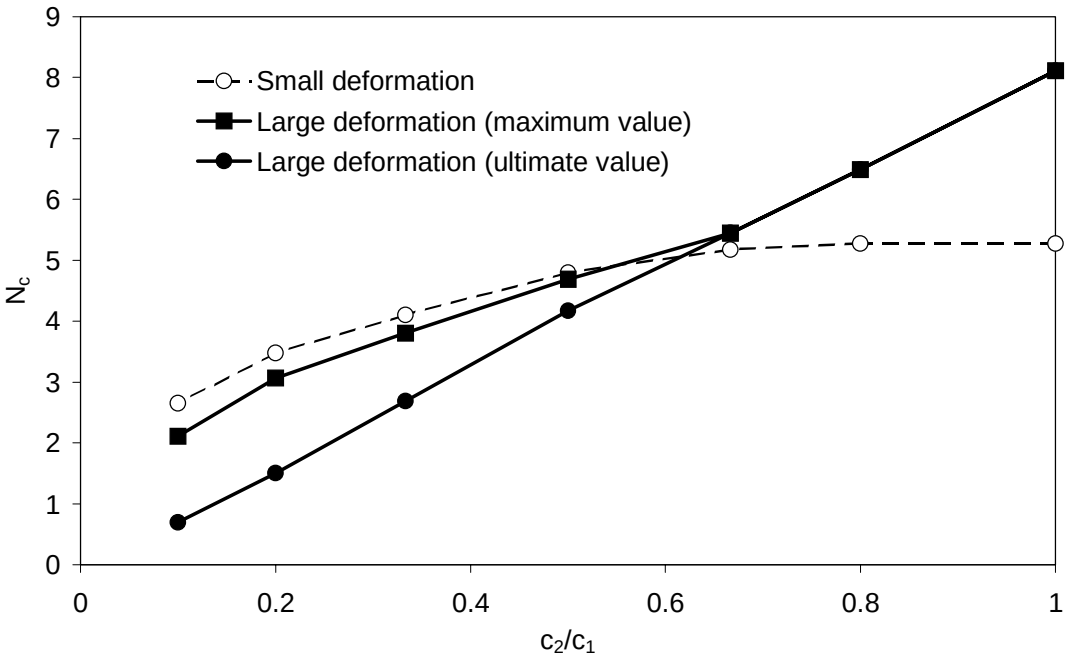

(b) H/B = 1

Figure 6 Bearing capacity factors for a strip footing

(large deformation analysis)

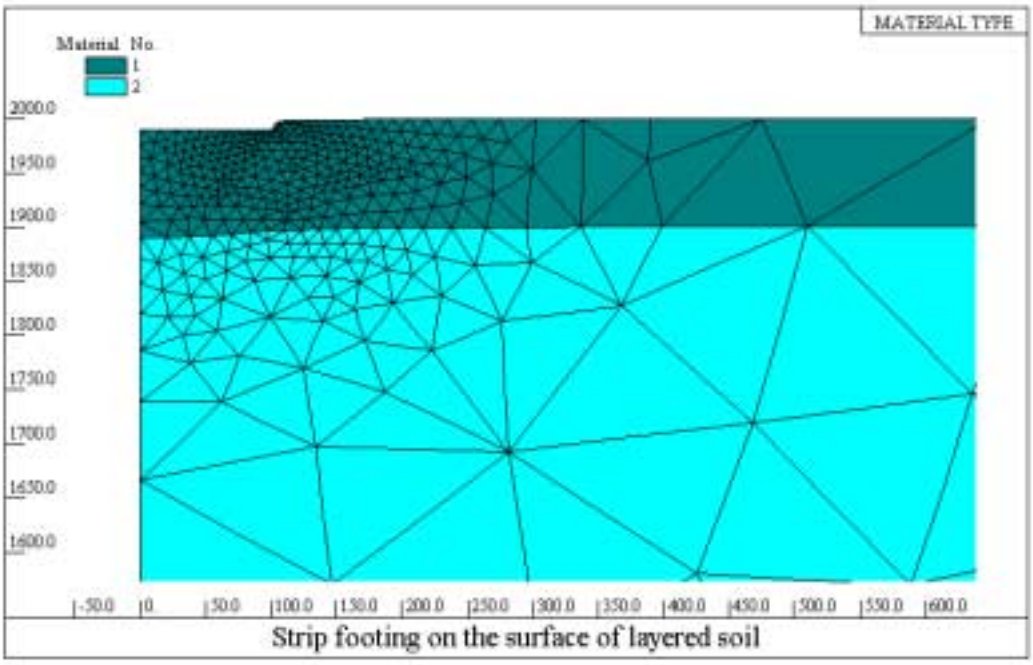

(a) s/B = 5%

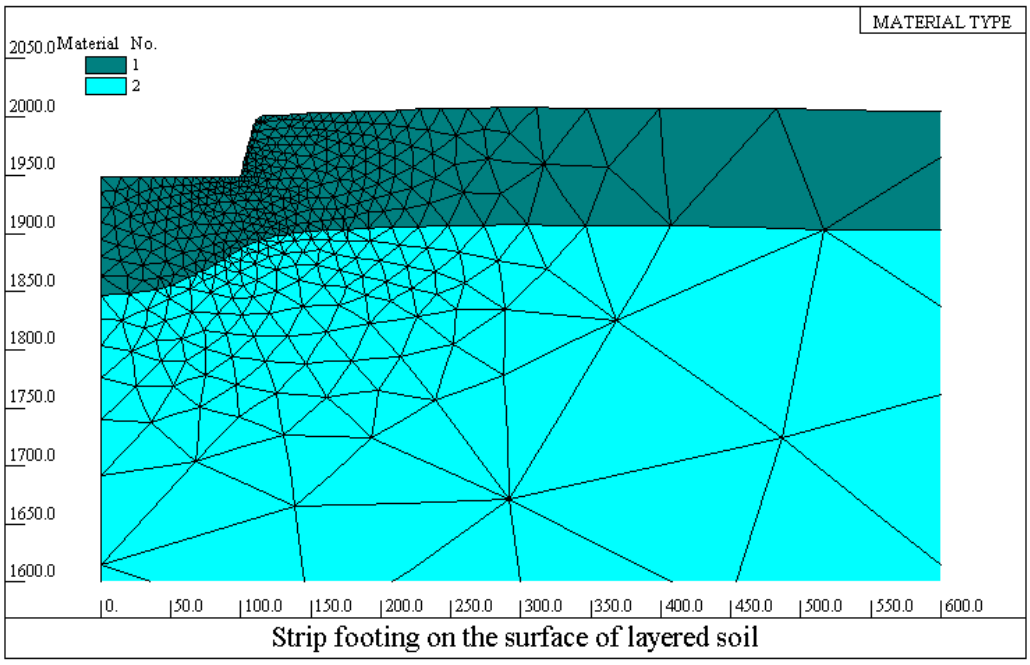

(b) s/B = 25%

Figure 7 The process of large penetration of strip footing into layered soil

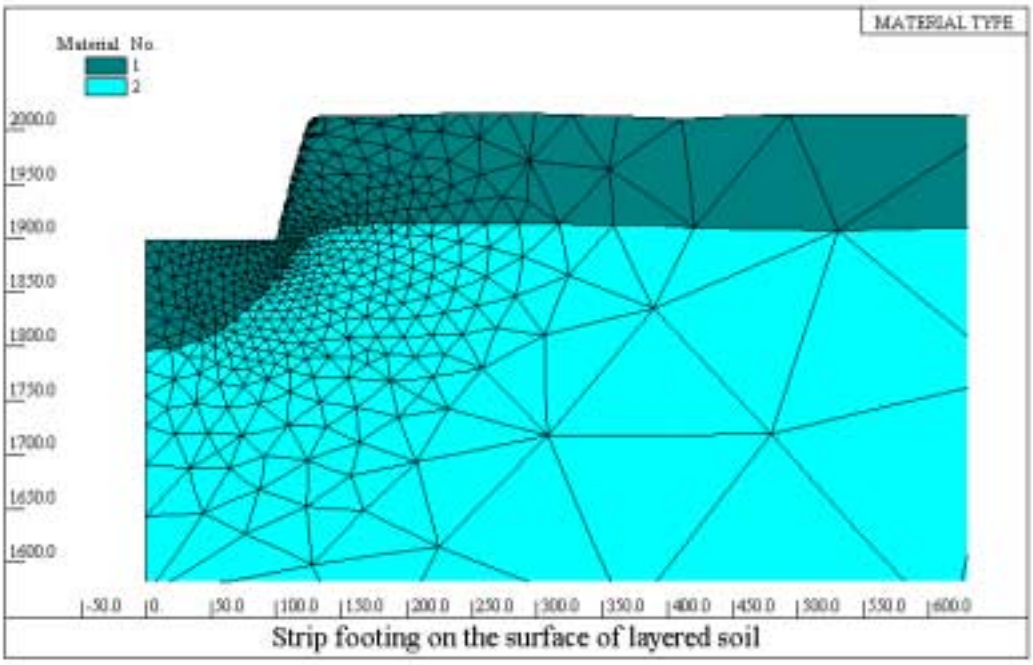

(c) s/B = 50%

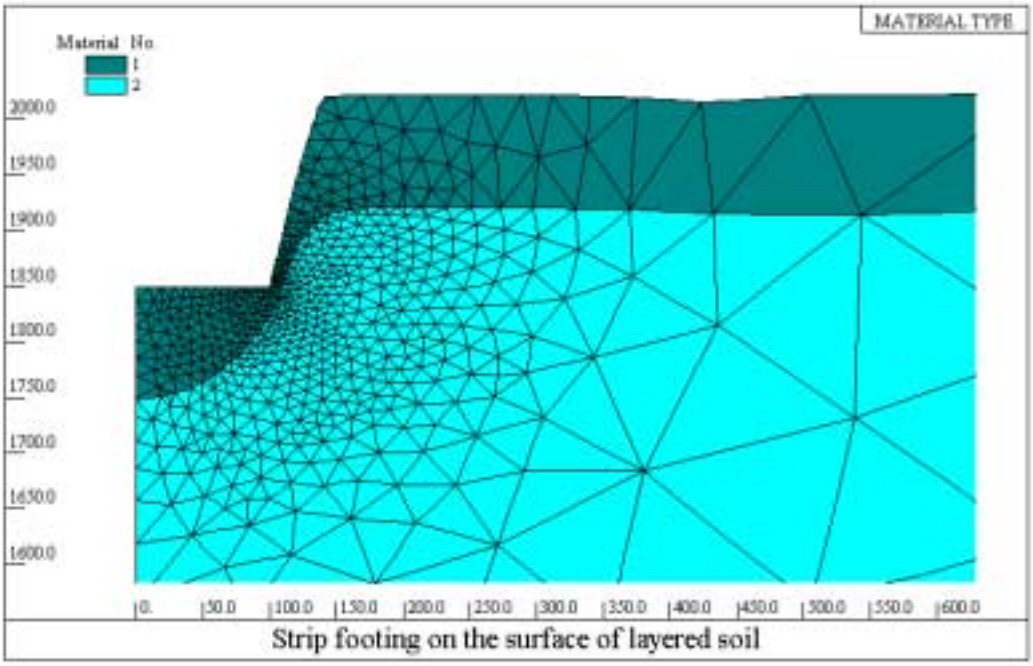

(d) s/B = 75%

Figure 7 The process of large penetration of strip footing into layered soil

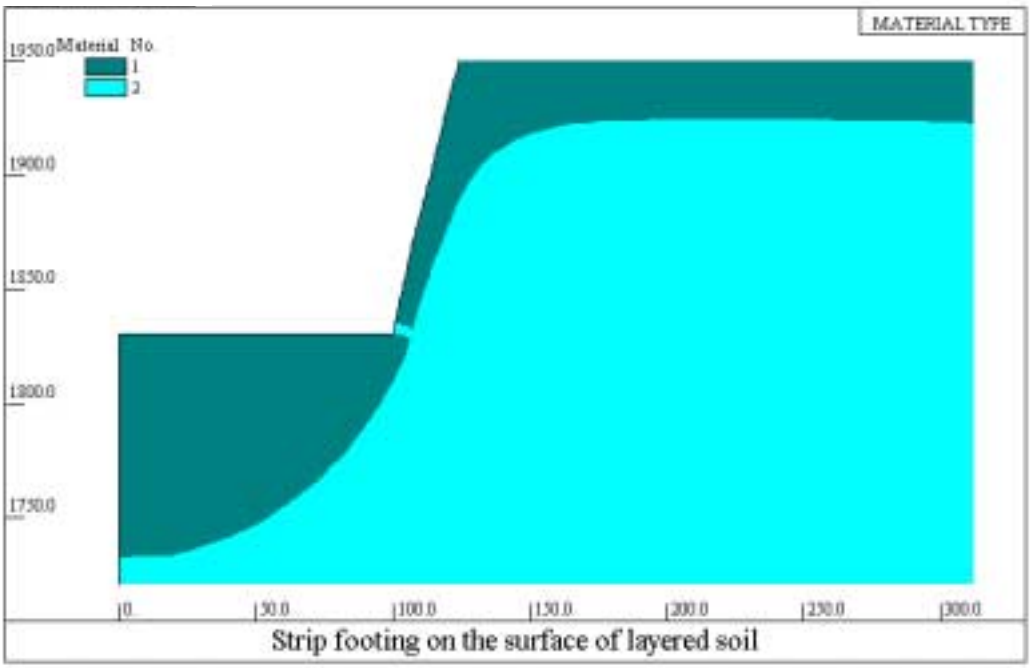

(e) s/B = 85%

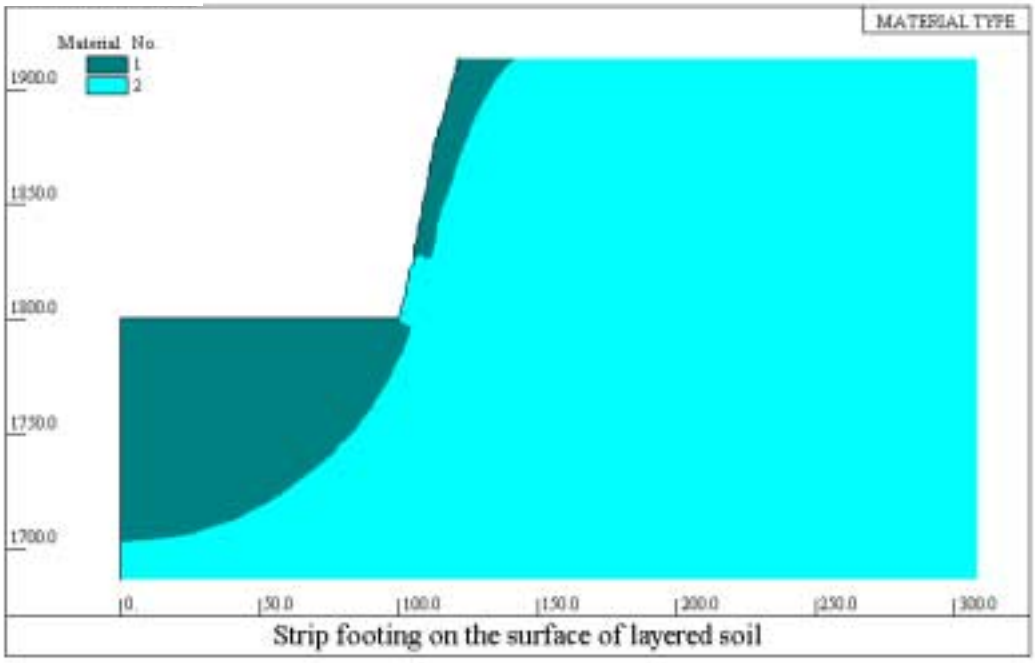

(f) s/B = 100%

Figure 7 The process of large penetration of strip footing into layered soil

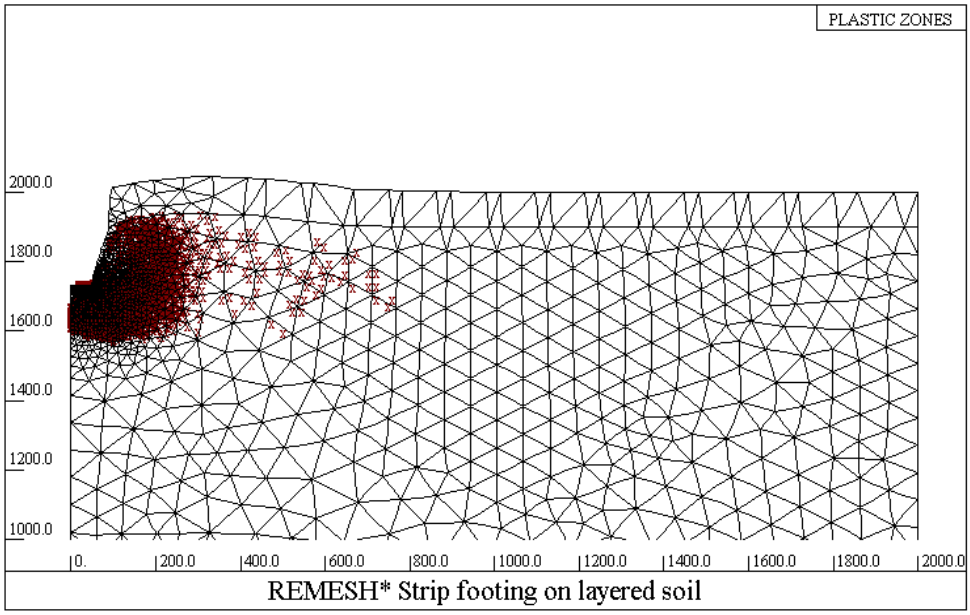

(a) c_2/c_1=0.5 (s/B = 2.6)

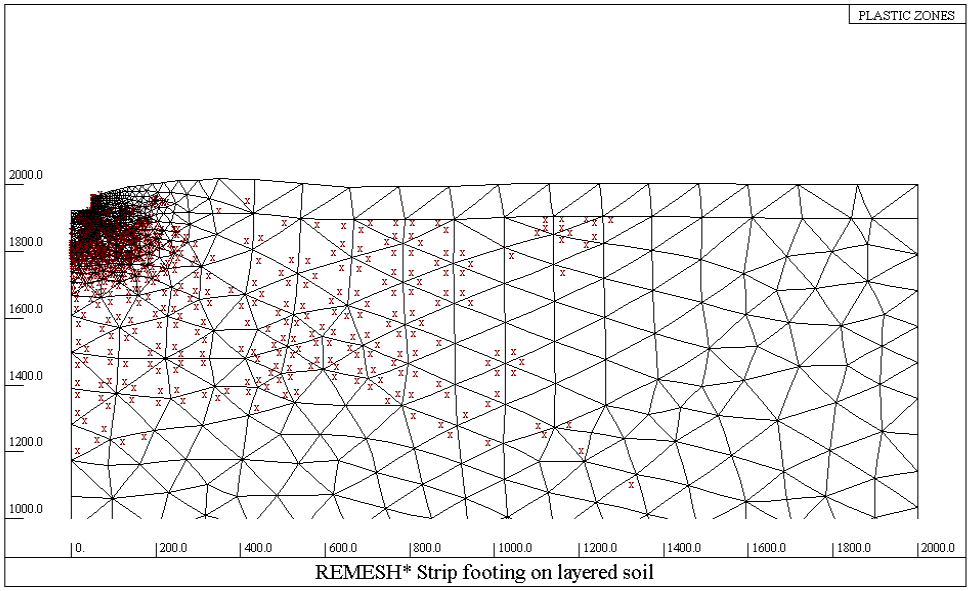

(b) c_2/c_1 = 0.1 (s/B = 0.8)

Figure 8 Plastic zones developed in layered clay due to penetration of a strip footing (H/B = 1)

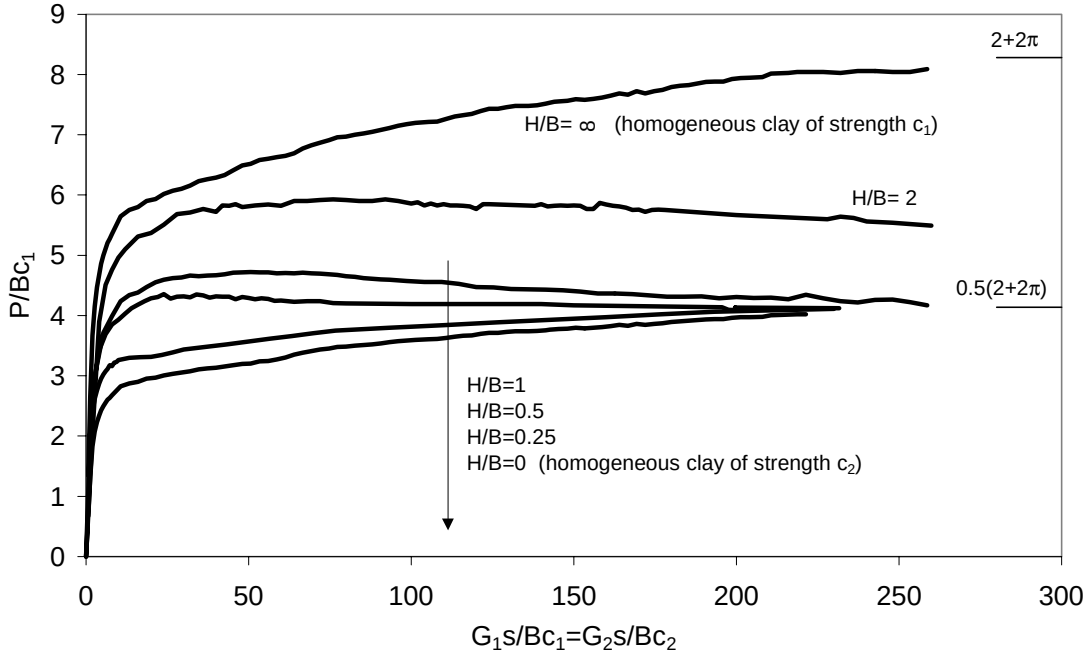

Figure 9 Effect of H/B on load-displacement behaviour ($c_2/c_1 = 0.5$)

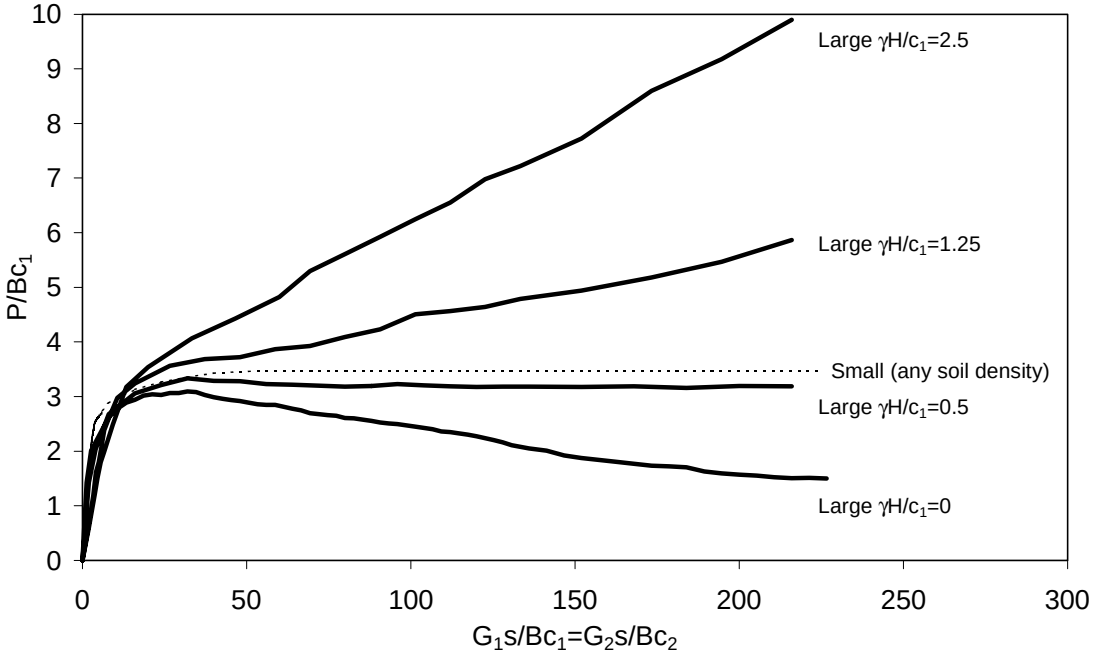

(a) c_2/c_1 = 0.2, H/B = 1

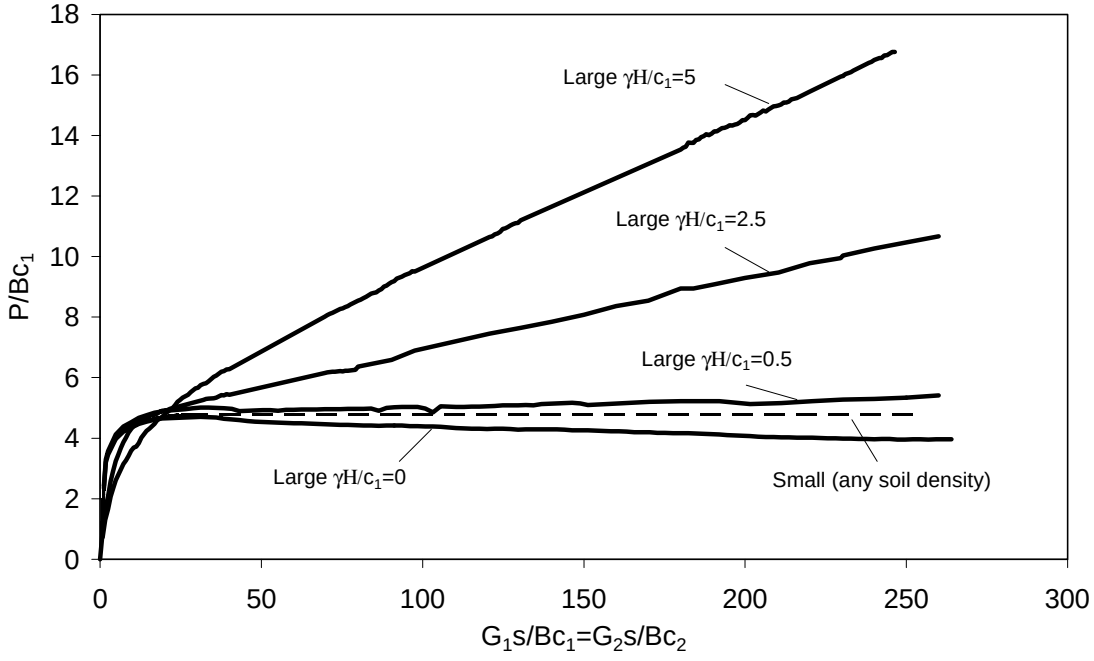

(b) c_2/c_1 = 0.5, H/B = 1

Figure 10 Effect of soil density on load-displacement behaviour

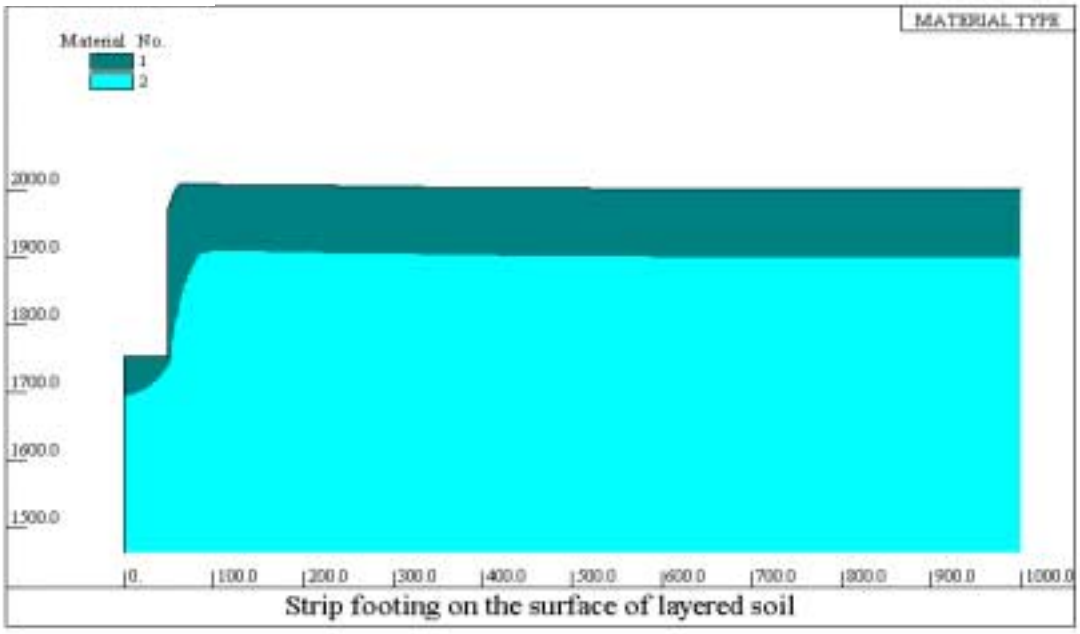

(a) Considering soil weight

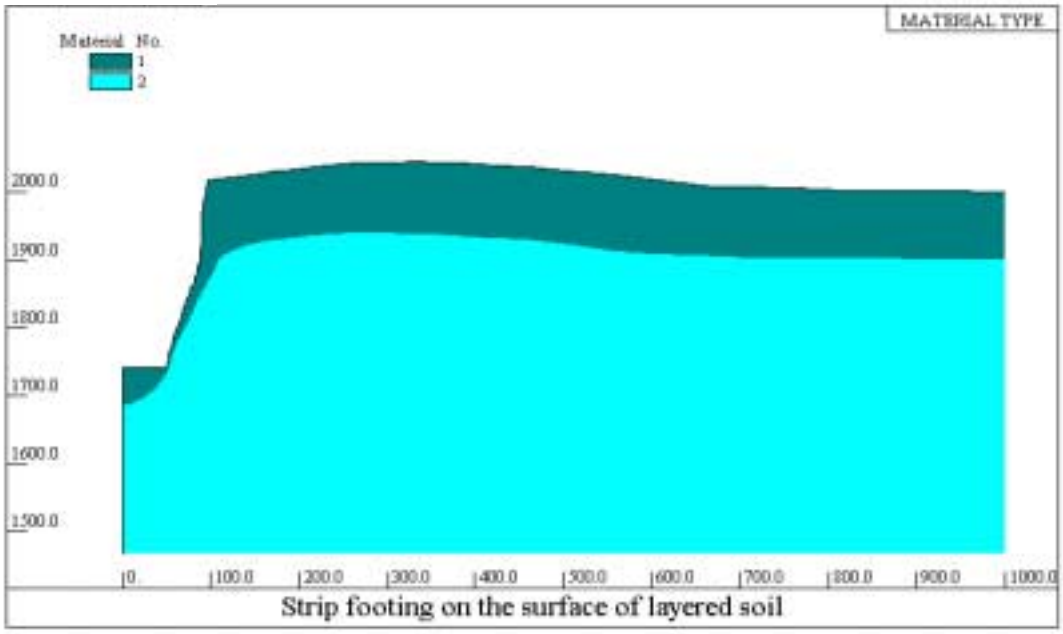

(b) Without considering soil weight

Figure 11 Effects of soil self-weight (s/B = 2.5, H/B = 1, c_2/c_1 = 0.5)

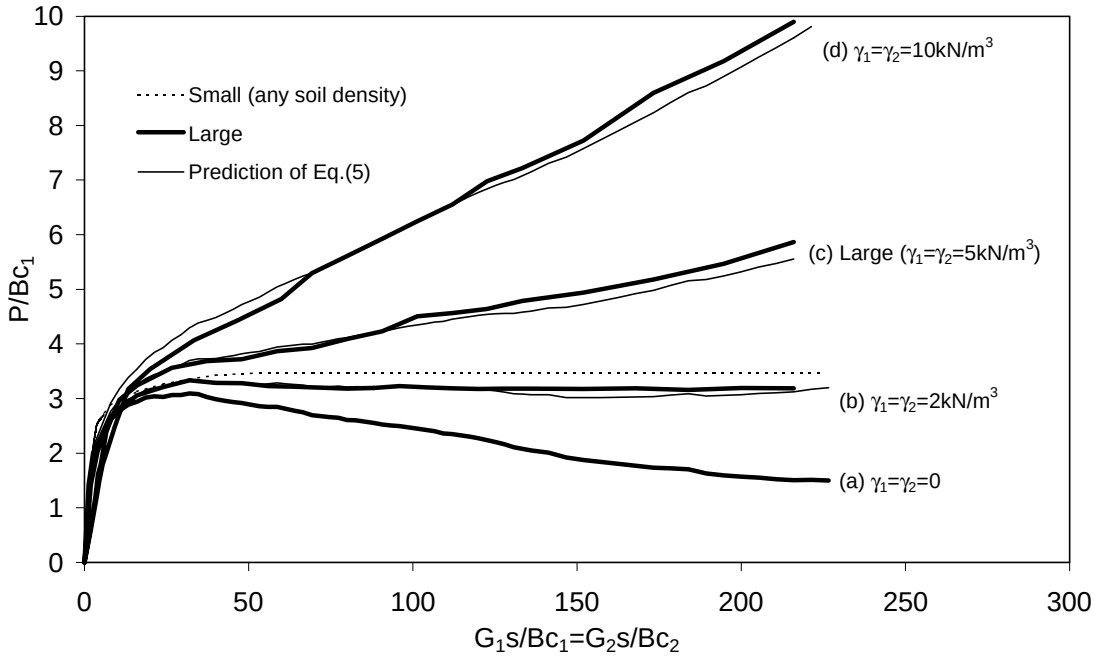

(a) $c_2/c_1 = 0.2$, H/B = 1

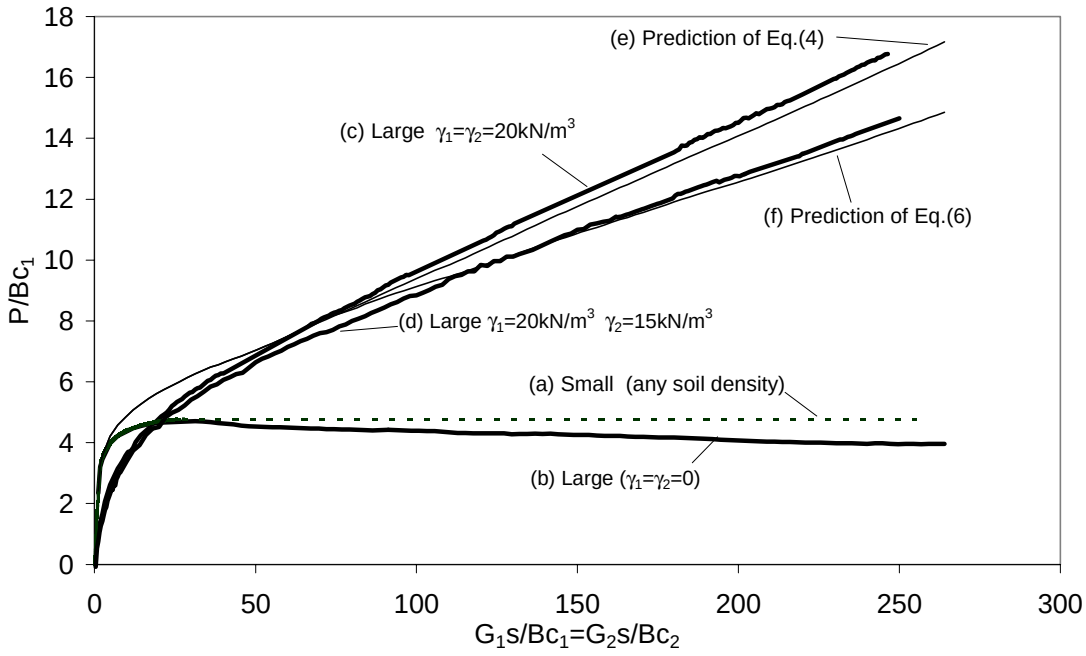

(b) $c_2/c_1 = 0.5$, H/B = 1

Figure 12 Load-settlement curves of a strip footing penetrating into layered clay of various soil densities

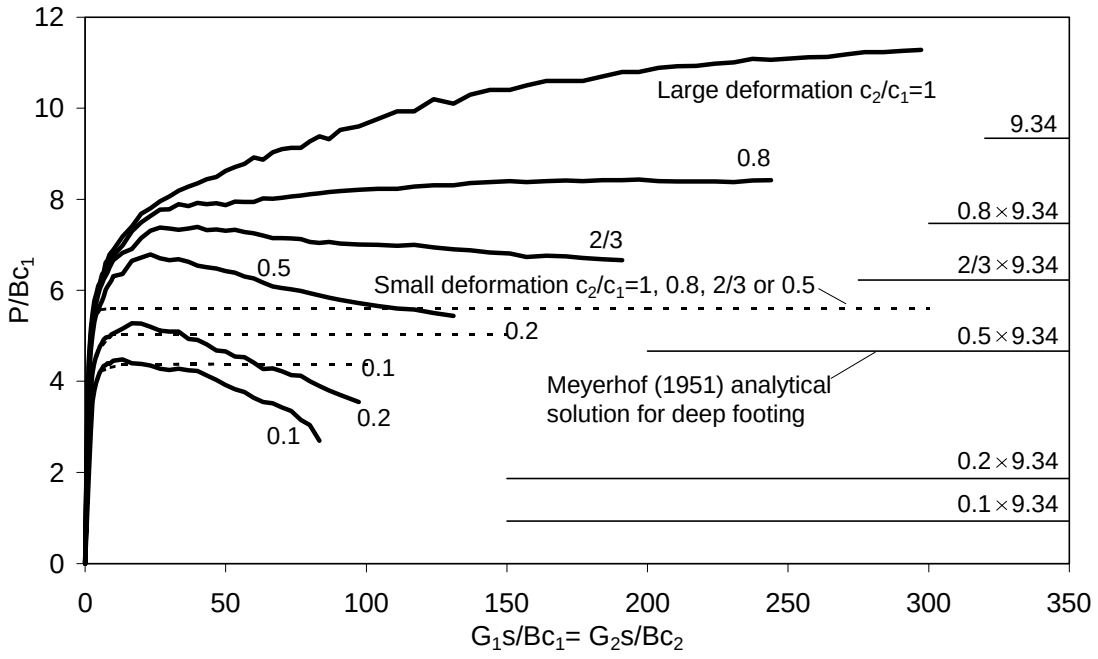

Figure 13 Typical normalized load-settlement curves for a circular footing penetration into layered clay (H/B = 1)

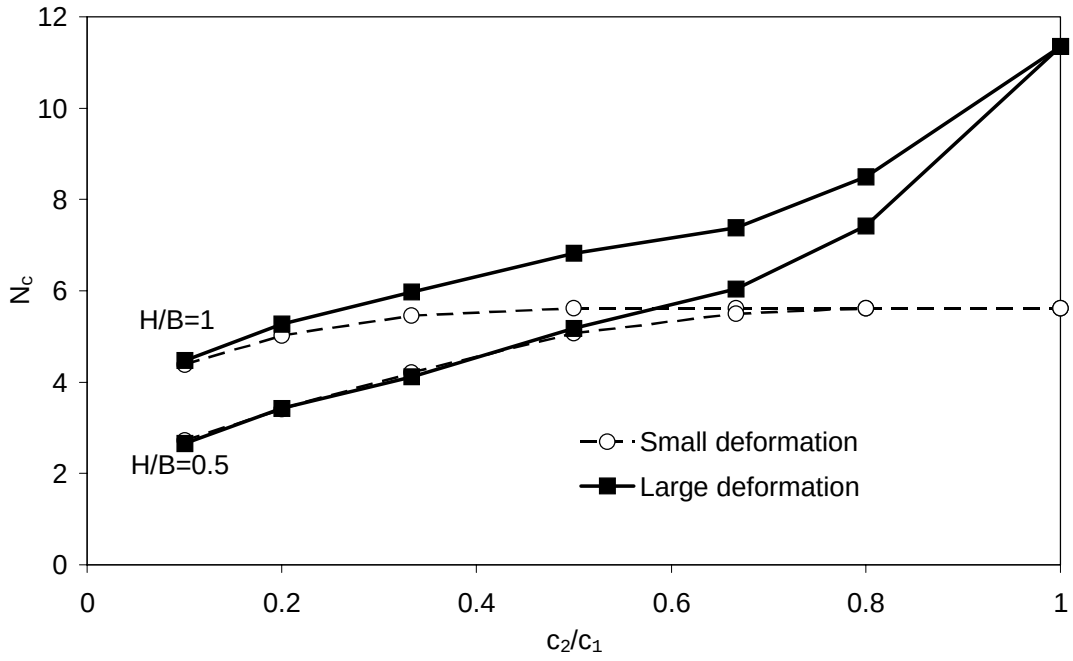

Figure 14 Bearing capacity factors of layered clay under a circular footing (large deformation)

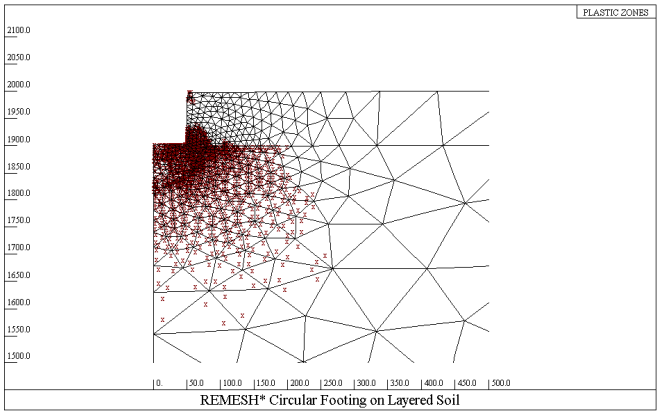

(a) $c_2/c_1 = 0.1$

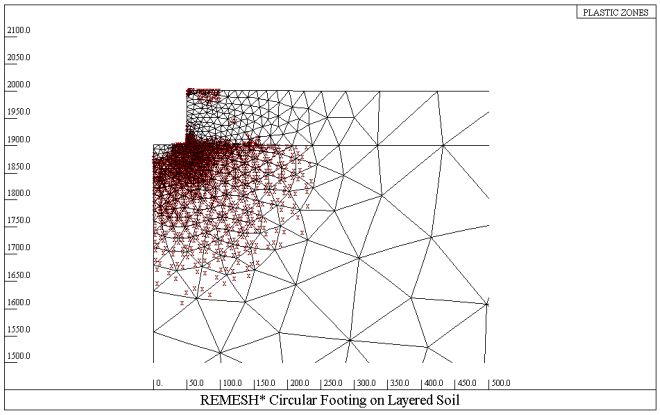

(b) $c_2/c_1 = 0.5$

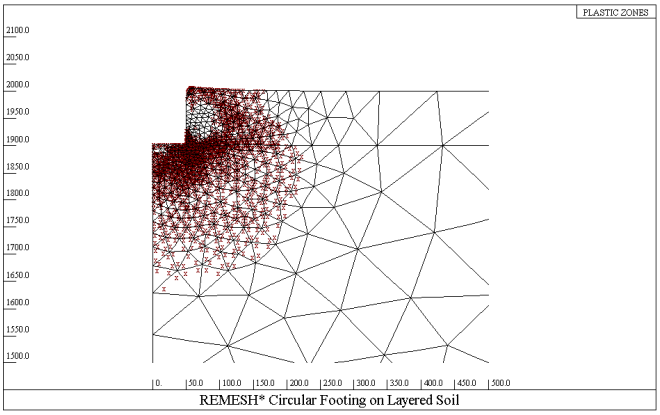

(c) $c_2/c_1 = 0.8$

Figure 15 Plastic zones developed in layered clay due to penetration of a circular footing (H/B = 1, s/B = 1)